

## New Thyristor Platform for UHVDC (>1 MV) Transmission

J. Vobecký, T. Stiasny, V. Botan, K. Stiegler, U. Meier, ABB Switzerland Ltd, Semiconductors, Lenzburg, Switzerland, jan.vobecky@ch.abb.com

M. Bellini, ABB Corporate Research Center, Dättwil, Switzerland

### Abstract

New thyristor platform with voltage ratings 6.7 kV, 7.2 kV and 8.5 kV was developed to enable an optimal design of converter valves with the DC link rating voltages over 1000 kV. Silicon resistivity and wafer thickness were chosen to fulfill the demands laid on the blocking capability of UHVDC application. A proper choice of electron irradiation energy and dose for  $Q_{rr}$  banding provides the optimal technology curve between the  $V_T$  and  $Q_{rr}$ . Full utilization of six inch wafers and the optimized layout of amplifying gate and cathode improved the ON-state current ratings by  $\approx 20\%$  compared to prior art thanks to the reduced ON-state voltage by  $\approx 10\%$ . Together with the low value of circuit commutated recovery time  $t_q$ , the new thyristor platform provides more efficient and stable converter valves for the next generation UHVDC systems to be operated at the rating power breaking the level of 10 GW.

### 1. Introduction

Since 1954, the high-voltage direct current (HVDC) transmission technology demonstrates its advantages over the alternating current (AC) solutions. It is about a more precise control of power flow and hence better grid stability, much lower power losses over very long distances, narrower transmission corridor, possibility of underground and underwater transmission, etc. These advantages were confirmed by numerous HVDC projects carried out in recent years. A common trend in the HVDC field is the continuous increase of transmitted power and the efficiency of transmission. In 2011, this trend resulted in the ultra high-voltage DC (UHVDC) system with rated DC voltage of  $\pm 800$  kV and rating power of 6400 MW transmitted over 1980 km line in China [1, 2].

The requirement of even higher transmitted power over long distances stimulates the development of new systems with rated DC voltages over 1 MV and higher current ratings. This lays new demands on the phase controlled thyristor (PCT) for inverter valves which have to provide higher rated current for the same blocking voltages. To fulfill this demand, the

PCTs with lower ON-state voltages ( $V_T$ ) for equivalent turn-OFF losses are needed. Since the PCT is non-punch-through device, higher blocking voltages require thicker silicon, which increases the  $V_T$ . Assuming the same thermal resistance of available package, the maximal rating current then decreases accordingly. Therefore, the optimal voltage class of PCT for given valve target parameters can be rigorously chosen only when the electrical ratings of neighboring voltage classes are precisely known. The aim of this paper is to present the new six inch PCT platform comprising the voltage classes 6.7, 7.2 and 8.5 kV with improved ratings of ON-state current, which facilitates this optimization.

## 2. Device Design and Processing

Recently, the reproducible processing of 6" PCTs with repetitive peak blocking voltages up to 8.5 kV has been shown possible. Prerequisite for this is the usage of FZ NTD silicon wafers subsequently subjected to advanced diffusion techniques, which provide the required purity after long-running diffusion [2, 3]. An additional improvement in ratings can be yielded by further optimization of silicon resistivity and thickness, silicon area utilisation, lateral structuring of amplifying gate and cathode shorts and lifetime control for the banding of reverse recovery charge  $Q_{rr}$ . The choice of resistivity and thickness implies the classical judgement of punch-through and avalanche effects with simultaneous consideration of the impact of cosmic rays. The anode and cathode area can be enlarged, if homogeneous diffusion up to the very edge of a wafer is assured. The cathode area can be further optimized using an effective shorting pattern and amplifying gate.

Also a sufficiently high energy of electron irradiation can give more favourable injection dependence of excess carrier lifetime  $\tau$  as shown in Fig.1. These curves were calculated from the Shockley-Read-Hall (SRH) model for generation-recombination rate of electrons  $R_n$

$$R_n = \sum_{i=1}^m \left[ c_{ni} \cdot n \cdot N_{ti} \cdot (1 - f_i) - e_{ni} \cdot N_{ti} \cdot f_i \right] \quad , \quad (1)$$

where  $m$  is the amount of deep levels,  $n$  is the electron concentration,  $N_{ti}$  ( $\text{cm}^{-3}$ ) is the concentration of  $i$ -th deep level and  $c_{ni}$  and  $e_{ni}$  are respectively the capture and emission coefficients of electrons of  $i$ -th deep level.  $f_i$  is the occupation probability of  $i$ -th deep level

$$f_i = \frac{n_{ti}(x)}{N_{ti}(x)} \quad , \quad (2)$$

where  $n_{ij}$  is the concentration of electrons at  $i$ -th deep level. The resulting lifetime of excess electrons as shown in Fig.1 then reads

$$\tau_n = \frac{\Delta n}{R_n} \quad (3)$$

When the parameters  $c_{ni}$  and  $e_{ni}$  of the model above are properly calibrated for different energy of electron irradiation [4] and the calibrated SRH model is used in device simulator, a better technology curve can be found for the higher energy of electron irradiation as is shown in Fig. 2. This is because the low irradiation energy results in much lower concentration ratio of divacancies (V-V:  $E_c - 0.42$  eV) to vacancy-oxygen pairs (V-O:  $E_c - 0.16$  eV) than the high energy. Since the V-O pairs reduce the carrier lifetime mainly at high level injection, while the V-V do just opposite, the high energy electrons provide much better ratio between the low level ( $n < 10^{16}$  cm<sup>-3</sup>) and high level lifetimes (see  $n > 10^{16}$  cm<sup>-3</sup> in Fig.1). As the turn-off of a PCT is controlled mainly by the low level lifetime, the trade-off curve improves with increasing energy of electron irradiation provided that a proper post-irradiation annealing process is used.

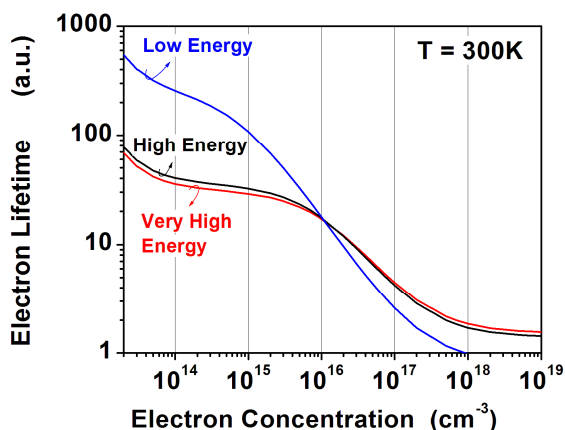


Fig.1: Simulated injection dependence of carrier lifetime for 8.5 kV PCT using the SRH model accounting for a different energy of electron irradiation.

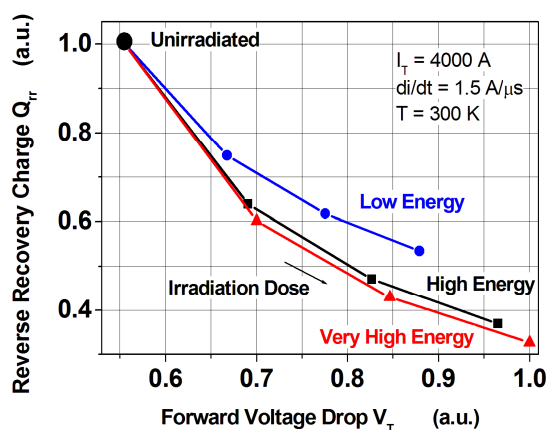


Fig.2: Technology curves for 8.5 kV PCT with different energy of electron irradiation resulting from the calibrated device simulation.

### 3. Experimental Results

Fig.3 shows that the measured forward and reverse blocking characteristics of new devices have the margin required for the classical HVDC application. In addition to the usual

repetitive peak blocking voltage under both forward and reverse biases ( $V_{DRM}$ ,  $V_{RRM}$ ), PCT can be exposed to non-repetitive peak reverse avalanche voltage, which is significantly higher than  $V_{RRM}$ . Relatively high currents are allowed to flow through the device, which is biased to the knee of the reverse I-V curve. The junction termination and its passivation is designed to be enough robust for this mode of operation.

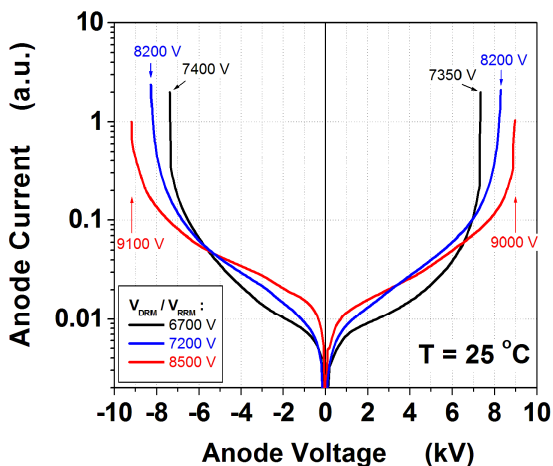


Fig.3: Blocking characteristics of PCTs for voltage classes 6.7, 7.2 and 8.5 kV.

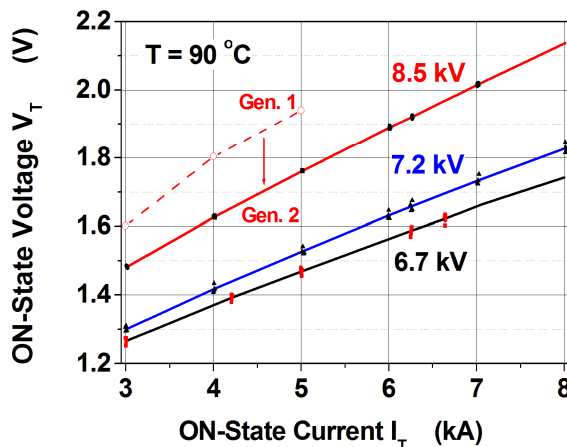


Fig.4: ON-state voltage drop vs. ON-state current for voltage classes 6.7, 7.2 and 8.5 kV.

Fig.4 shows the measured dependence of  $V_T$  on  $I_T$  for all three voltage classes including the improvement for the 8.5 kV devices against the first 6" PCT called *Generation 1* [2]. The devices are electron irradiated to the dose, which assures the reverse recovery charge  $Q_{rr}$  according to specification. The  $Q_{rr}$  - banding for the HVDC application is relatively narrow in order to achieve a uniform distribution of voltage between the individual serially connected devices otherwise additional devices would have to be added into the stack to compensate for a higher voltage distribution over the valve. The higher wafer thickness necessary to achieve the nominal blocking voltage of 8.5 kV increases the  $V_T$  above 1.7 V already at  $I_T \approx 5$  kA. Consequently, the rating current of 8.5 kV class is reduced to  $I_{Tmax} = 5$  kA to avoid reaching the limit of cooling system. This value is still by 20 % higher compared to the *Generation 1* thanks to by  $\approx 10\%$  lowered  $V_T$  [1, 2]. On the other hand, both the 6.7 and 7.2 kV classes can be specified up to  $I_{Tmax} \approx 6.5$  kA.

The trade-off curves between the  $V_T$  and  $Q_{rr}$  are shown for  $I_T = 6.25$  kA in Fig.5. The upper left points correspond to as processed devices. Using the electron irradiation the device parameters move to the  $Q_{rr}$  band according to target specification, i.e. towards the lower right end. The dashed curve for the 8.5 kV voltage class was measured for the maximal current

rating of  $I_T = 5$  kA. The ON-state voltage for this device is  $V_T \approx 1.75$  V at  $I_T = 5$  kA and  $T = 90$  °C, which is already close to the curve achieved for the 7.2 kV voltage class at  $I_T > 6$  kA. The value of  $V_T$  can be further adjusted by choosing an optimized  $Q_{rr}$  band according to the priorities of given application.

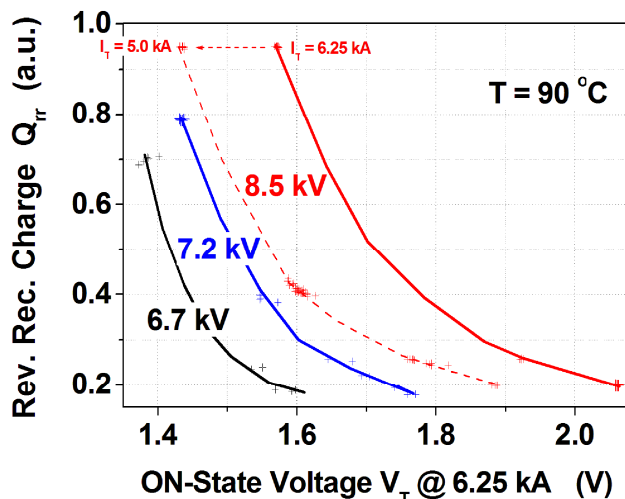


Fig.5: Trade-off curves between  $V_T$  and  $Q_{rr}$  for voltage classes 6.7, 7.2 and 8.5 kV.

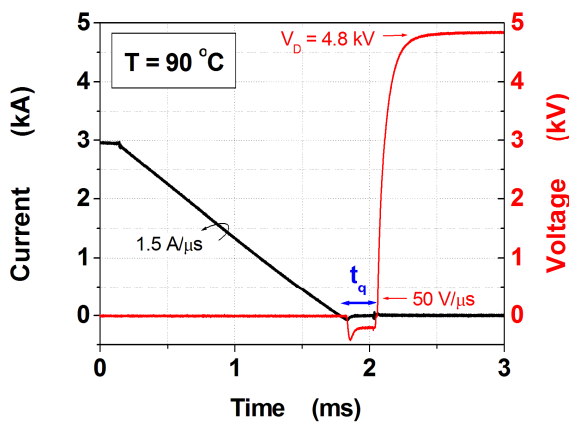


Fig.6: Single shot example from measurement of circuit commutated recovery time  $t_q$  for 8.5 kV device.

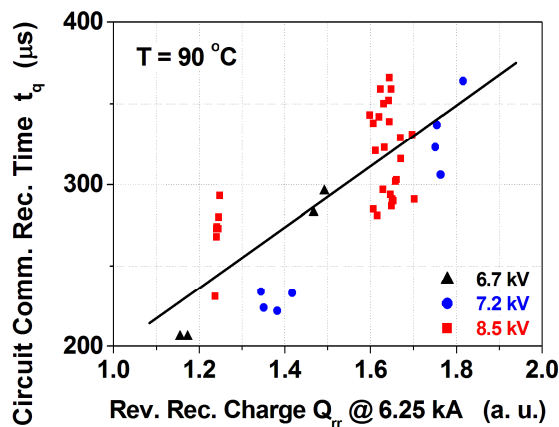


Fig.7: Circuit commutated recovery time  $t_q$  vs. reverse recovery charge  $Q_{rr}$ .

The circuit commutated recovery time  $t_q$  is the most relevant dynamic parameter, because it supports the stability of network system by enabling the power flow flexibly responding to sudden changes in demand. Fig.6 shows one of the measurement conditions of  $t_q$ . Here the 8.5 kV device is commuted from the ON-state current of  $I_T = 3$  kA at  $T = 90$  °C by reverse

voltage of  $V_R = 200 \text{ V}$  with  $di/dt = 1.5 \text{ A}/\mu\text{s}$  and after the time  $t \geq t_q$  it is forward biased to  $V_D = 4800 \text{ V}$  with the voltage rate of rise  $dv/dt = 50 \text{ V}/\mu\text{s}$ . While for  $t < t_q$  the device does not block and eventually returns to the ON-state (not shown here), for  $t \geq t_q$  the device remains safely in the forward blocking regime as shows the Fig.6. Fig.7 illustrates the dependence of  $t_q$  on the reverse recovery charge  $Q_{rr}$  measured in the conditions of the Fig.6. The magnitudes of  $Q_{rr}$  are in the  $Q_{rr}$  band or in its proximity and were obtained by varying the dose of electron irradiation. This means that for all the PCTs within technical specification the magnitude of  $t_q$ , was measured well below  $500 \mu\text{s}$ . Such a low value provides the above mentioned stability and flexibility of HVDC system with sufficient margin.

## 4. Conclusions

New PCT platform with repetitive peak blocking voltages of 6.7, 7.5 and 8.5 kV provides devices for the next generation converter valve with significantly increased transmitted DC power compared to previous generation. This is possible thanks to the significant improvement of key device parameters for UHVDC transmission system, which are  $V_T - Q_{rr}$  technology curve, maximal rated current and  $t_q$ . The overall improvement allows us to introduce the second generation of six inch UHVDC PCT technology, where valve designers can choose between the maximal rating current up to  $I_T \approx 6.5 \text{ kA}$  with more serially connected 6.7 or 7.2 kV PCTs or up to  $I_T \approx 5 \text{ kA}$  with less 8.5 kV serially connected PCTs. This enables one to design more energy efficient converter valves for the next generation UHVDC systems to be operated even at the rating power breaking the level of 10 GW.

## 5. References

- [1] J. Waldmeyer, W. Zhengming, Six Inch Thyristors for UHVDC, IEC/CIGRE UHV Symposium, Beijing, 2007, pp.1 – 8.
- [2] V. Botan, J. Waldmeyer, M. Kunow, K. Akurati, Six Inch Thyristor for UHVDC Transmission, Proceedings PCIM 2010, Nuremberg, pp.476 – 479.
- [3] J. Przybilla, J. Dorn, R. Barthelmes, R. Joerke, U. Kellner-Werdehausen, Reaching New Limits with High Power Bipolar Devices, Proceedings PCIM 2010, Nuremberg, pp.761 – 766.
- [4] J. Vobecky, P. Hazdra, O. Humbel, N. Galster, Crossing Point Current of Electron and Proton Irradiated Power P-i-N Diodes, Microelectronics Reliability 40, 2000, pp.427 – 433.